

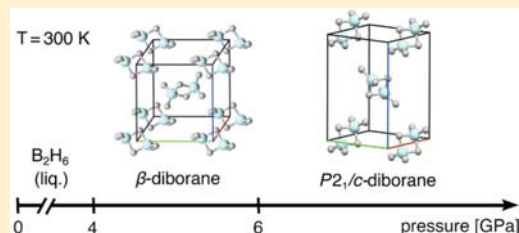
Pressure-Induced Polymorphic Transitions in Crystalline Diborane Deduced by Comparison of Simulated and Experimental Vibrational Spectra

Amin Torabi, Yang Song, and Viktor N. Staroverov*

Department of Chemistry, The University of Western Ontario, London, Ontario N6A 5B7, Canada

Supporting Information

ABSTRACT: We investigate and assign the pressure-induced structural transformations in crystalline diborane (B_2H_6) observed spectroscopically by Song and co-workers (*J. Phys. Chem. B* **2009**, *113*, 13509; *J. Chem. Phys.* **2009**, *131*, 174506) between 3.5 and 24 GPa at room temperature. The assignment is made by calculating the Raman and infrared vibrational spectra of 10 candidate structures at various pressures and comparing the results to experiment. We find that solid diborane undergoes a polymorphic transition at about 6 GPa from β -diborane ($P2_1/n$) to a $P2_1/c$ diborane and possibly a second transition near 14 GPa to another $P2_1/c$ diborane structure. We conclude that no cyclic oligomers or chains of the composition $(BH_3)_n$ ($n > 2$) are formed from diborane up to at least 24 GPa under the experimental conditions employed by the Song group, even when such structures are thermodynamically favored. This suggests that pressure-induced chemical transformations of molecular crystals of diborane are kinetically hindered.



INTRODUCTION

Diborane (B_2H_6) is the simplest stable molecular boron hydride.¹ An electron-deficient species, B_2H_6 has an unusual gas-phase structure² in which the boron atoms are held together by two three-center two-electron B–H–B bonds. At ambient conditions, diborane is a gas (mp = 108 K, bp = 181 K at 1 atm), but it can be liquefied and solidified by cooling or compression. Solid phases of diborane, especially at high-pressure conditions, have been identified as possible high-temperature superconductors³ and hydrogen-storage media with a storage density exceeding that of liquid H_2 .⁴ Experimental and theoretical investigations of high-pressure structures and transformations of boron hydrides are therefore of significant technological interest.

At present, experimental information about crystalline boron hydrides is very limited due to the difficulty of locating weakly scattering hydrogen and boron atoms by X-ray diffraction techniques. At low temperatures ($T < 100$ K) and ambient pressure, only four forms of B_2H_6 have been reported in the literature,^{5,6} and only one of them, β -diborane, has been identified and characterized.⁷ The β -phase crystallizes in the $P2_1/n$ space group (monoclinic crystal system), with two formula units per cell,⁷ as shown in Figure 1.

Even less is known about high-pressure phases of solid boron hydride. In 2009, the Song group^{8,9} studied pressure-induced structural transformations of diborane at room temperature using in situ Raman and synchrotron infrared (IR) spectroscopy. On the basis of changes in spectral profiles of B_2H_6 between 1 atm and 24 GPa, it was suggested that diborane undergoes three phase transitions at about 4, 6, and 14 GPa. The first of these is from the liquid to the solid state, and the

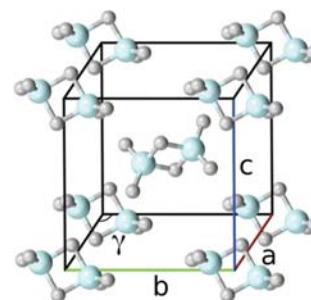


Figure 1. Structure of β -diborane at ambient pressure ($a = 4.416$ Å, $b = 5.963$ Å, $c = 6.069$ Å, $\gamma = 104.2^\circ$). The lattice parameters were optimized using the PBEsol functional.

other two are polymorphic transitions. The structures of the crystalline phases involved in the polymorphic transitions, however, have not been identified.

In 2011, Yao and Hoffmann¹⁰ carried out an extensive theoretical investigation of possible pressure-induced transformations of boron hydride between 1 atm and 100 GPa using the Perdew–Burke–Ernzerhof¹¹ (PBE) functional. These workers considered several plausible polymorphs including structures consisting of dimers, cyclic trimers, tetramers, and hexamers of the general formula $(BH_3)_n$, as well as crystals of one-dimensional infinite chains of BH_3 . By comparing the calculated enthalpies of these structures at various pressures,

Received: October 10, 2012

Revised: January 15, 2013

Published: January 16, 2013

Yao and Hoffmann predicted two phase transitions at 0 K: the first at ~ 4 GPa, from β -diborane to a molecular crystal of cyclic trimers crystallizing in either the $Cmc2_1$ or the $P\bar{1}$ space group; the second at ~ 36 GPa, from the molecular crystal of trimers to a $P2_1/c$ crystal of one-dimensional chains, $(BH_3)_n$.¹⁰ The predictions of Yao and Hoffmann are consistent with the local-density-approximation (LDA) calculations by Barbee et al.⁴ which also suggested that molecular forms of boron hydride become unstable at high pressure. One should keep in mind that these predictions were made theoretically by considering only the relative thermodynamic stability (enthalpies) of various phases, leaving aside the issue of kinetic persistence, and that the post-2009 computational studies of crystalline diborane^{3,10} did not fully exploit the experimental data of Song and co-workers.^{8,9}

In this paper, we interpret the structural changes in compressed diborane observed spectroscopically by the Song group.^{8,9} We do this by calculating the frequencies and intensities of Raman and IR transitions for the 10 candidate structures listed in Table 1 and comparing the results to the

Table 1. Candidate Structures of Crystalline Boron Hydride Used for Spectroscopic Assignment in This Study

structure	molecular unit	source
β -diborane	dimer	ref 7, $P2_1/n$
$P2_1/c$ (A)	dimer	ref 10, $P2_1/c$ (1)
$P2_1/c$ (B)	dimer	ref 3
$Cmc2_1$	trimer	ref 10
$P\bar{1}$	trimer	ref 10
$P2_1/c$	chain	ref 10, $P2_1/c$ (2)
$Pna2_1$	chain	ref 3
$P2_1/m$	chain	ref 3
$Pbcn$	chain	ref 3
$Cmcm$	chain	ref 3

observed spectra. We selected these structures because, to the best of our knowledge, they are the only ones for which full structural parameters have been published in the literature.^{3,7,10}

The main difference between the computational methodology adopted in this work and those of the previous studies^{3,4,10} is that here we go beyond the LDA and PBE approximation and use the Perdew–Burke–Ernzerhof exchange–correlation functional for solids¹² (PBEsol), a minor but critical modification of the PBE¹¹ functional. We chose the PBEsol functional because it makes the most accurate prediction for the lattice parameters of the best-studied phase (β -diborane) at low temperature and ambient pressure (predicted: $a = 4.416$, $b = 5.963$, $c = 6.069$ Å, $\gamma = 104.2^\circ$; experiment:⁷ $a = 4.40$, $b = 5.72$, $c = 6.50$ Å, $\gamma = 105.1^\circ$) and is supposed¹² to become increasingly accurate at high pressures. The agreement between theory and experiment turns out to be sufficiently clear-cut to propose specific structure assignments.

COMPUTATIONAL METHODOLOGY

All calculations reported in this work were performed using Quantum ESPRESSO (version 4.3),¹³ a plane-wave/pseudopotential electronic structure code. The lattice parameters and atomic positions for each candidate structure were optimized at a fixed pressure at $T = 0$ K by minimizing the enthalpy. To simulate IR spectra, we optimized the candidate structures at the PBEsol level¹² and then calculated IR frequencies and intensities using the PBEsol functional. To simulate Raman

spectra, we reoptimized all structures at the LDA level and calculated Raman frequencies and intensities using the LDA. Different functionals had to be used for simulating IR and Raman spectra because Raman spectral intensities are implemented in Quantum ESPRESSO only for the LDA functional. In all cases, we used vibrational frequencies without applying any scale factors.

The pseudopotentials were taken from the Quantum ESPRESSO pseudopotential library.¹³ In the PBEsol calculations, the PBE ultrasoft Vanderbilt pseudopotentials¹⁴ with a cutoff energy of 90 Ry for the plane-wave expansion were utilized. In the LDA calculations, the norm-conserving LDA pseudopotentials with a cutoff energy of 130 Ry were employed. The Brillouin zone was sampled using the Monkhorst–Pack scheme.¹⁵ The following k -point meshes were used: $6 \times 4 \times 4$ for β -diborane; $6 \times 6 \times 4$ for the $P2_1/c$ (A) dimer and $P\bar{1}$ trimer; $6 \times 4 \times 6$ for the $P2_1/c$ (B) dimer and the $Pna2_1$, $Pbcn$, and $Cmcm$ chains; $4 \times 6 \times 4$ for the $Cmc2_1$ trimer; $4 \times 6 \times 6$ for the $P2_1/c$ chain; $6 \times 6 \times 6$ for the $P2_1/m$ chain. Convergence with respect to the cutoff energy and the k -point mesh was verified for all structures. The convergence criterion for Kohn–Sham self-consistency cycles was set to 10^{-10} Ry.

In all structural optimizations, the Broyden–Fletcher–Goldfarb–Shanno quasi-Newton algorithm was used for both ionic and cell dynamics. The optimization was stopped when the components of all Hellmann–Feynman forces dropped below 10^{-4} Ry/Å and the pressure on the cell was less than 0.05 GPa of the target. Lattice parameters and atomic positions optimized at each pressure were used as initial guesses for the optimization at the next higher pressure.

The nonresonant Raman intensities were computed using the method described in ref 16. IR intensities were calculated by density-functional perturbation theory.¹⁷ The XCrySDen package¹⁸ was used for visualizing the results.

RESULTS AND DISCUSSION

The lattice parameters and atomic positions for the 10 candidate structures optimized at 1 atm by the PBEsol method are listed in Table S1 of the Supporting Information. Figure 2 shows how the computed enthalpies of these structures vary with pressure. We see that β -diborane is *not* the most stable structure under compression. The trimer-based structures are more stable than β -diborane above ~ 0.5 GPa; the linear-chain

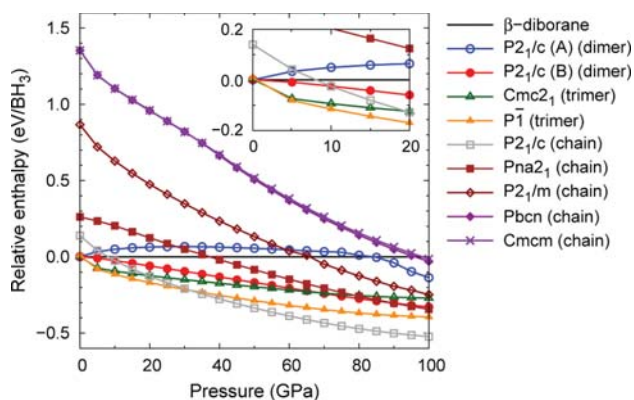


Figure 2. Enthalpies of the 10 candidate structures as functions of pressure, relative to the enthalpy of β -diborane. All enthalpies are calculated using the PBEsol functional.

$P2_1/c$ structure becomes the most favored above ~ 35 GPa. These observations are generally in agreement with the PBE calculations by Yao and Hoffmann¹⁰ and by Abe and Ashcroft.³ One noteworthy difference is that the PBEsol method predicts the two trimer structures ($Cmc2_1$ and $P\bar{1}$) to be almost as stable as β -diborane at ambient pressure (see the inset in Figure 2), whereas PBE calculations predict¹⁰ the trimers to have a slightly higher enthalpy than β -diborane until about 4 GPa (the difference is ~ 0.04 eV/ BH_3 at ambient pressure). Although such thermodynamic stability data are useful, they are not sufficient for making spectroscopic assignments. To cite a well-known example, diamond does not spontaneously turn into graphite at ambient temperature and pressure, even though the latter is favored thermodynamically.

In order to facilitate comparison with experiment, the Raman and IR spectra of the 10 candidate structures were calculated at the specific pressures for which the experimental data of refs 8 and 9 are available. It should be kept in mind that, at room temperature, diborane remains in the liquid state until ~ 3.5 GPa,^{8,9} so the experimental spectra recorded below this pressure cannot be directly compared to our calculations.

Raman Spectra. All experimental Raman spectra shown in this work are composite; that is, each was formed by combining three separate spectral regions from the original experimental work of ref 8: 100–1300, 1400–2400, and 2500–3000 cm^{-1} . The spectral region between 1300 and 1400 cm^{-1} was excluded because of intense Raman scattering by the diamond of the anvil cell. In the resulting composite spectra, arbitrary peak intensities within each window were scaled to approximately match the distribution of peak intensities in the simulated spectra. Frequencies below 700 cm^{-1} correspond to lattice modes; frequencies above 700 cm^{-1} are due to internal molecular vibrations.

Murli and Song⁸ found that the lowest-pressure solid phase of diborane (phase I) exists at room temperature between 3.5 and about 6 GPa. To identify this phase, we computed the Raman spectra of all candidate structures at 4.2 GPa and compared them to the experimental Raman spectrum recorded at the same pressure. The best agreement was found for β -diborane ($P2_1/n$), as shown in Figure 3 (for other structures,

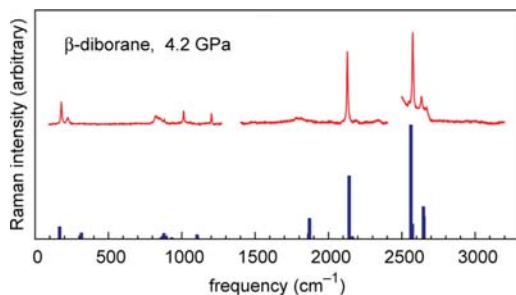


Figure 3. Experimental (red) and simulated (blue) Raman spectra of β -diborane at 4.2 GPa.

see Figure F1 and Table S1 in the Supporting Information). The most intense peaks in Figure 3 correspond to the terminal B–H symmetric stretching mode (ν_1). In the calculated spectrum, it occurs at 2562 cm^{-1} compared with 2574 cm^{-1} in the observed spectrum. The second most intense peak corresponds to the symmetric BHBH ring stretching (ν_2); it occurs at a lower frequency of 2141 cm^{-1} , compared to the experimental value of 2128 cm^{-1} . The calculated depolarization

ratio of these two modes is close to zero, as anticipated for totally symmetric modes. The antisymmetric terminal BH stretching (ν_{11}) is calculated to occur at 2647 cm^{-1} , in good agreement with the experimental value of 2633 cm^{-1} . The ring antisymmetric stretching mode (ν_6) is predicted to occur at 1871 cm^{-1} and was observed at 1813 cm^{-1} . Two lattice modes observed⁸ at 179 and 222 cm^{-1} are reproduced in our simulation at 167 and 246 cm^{-1} , respectively.

We note that the simulated Raman spectra of $P2_1/c$ (A) and $P2_1/c$ (B) diboranes are similar to the experimental spectrum at 4.2 GPa (see Figure F1 in the Supporting Information), but we rule out these structures because they have no lattice modes below 200 cm^{-1} (see Table S1 in the Supporting Information). The simulated spectra of the other seven candidate structures clearly do not match the experiment. The trimer and linear-chain structures consist of different molecular units, so their internal vibrational modes are very different from those of diborane molecules. All this allows us to conclude that phase I of ref 8 is β -diborane.

Upon compression of the sample to 6.4 GPa, Murli and Song⁸ observed the emergence of several new lattice and internal modes and interpreted them as evidence of a polymorphic transition from β -diborane to another phase referred to as phase II. As we argue below, these spectral changes are best reproduced by the calculated Raman spectrum of $P2_1/c$ (A) diborane. Just like β -diborane, the $P2_1/c$ (A) structure contains two B_2H_6 molecules per unit cell but has a different stacking of diborane molecules, depicted in Figure 4.

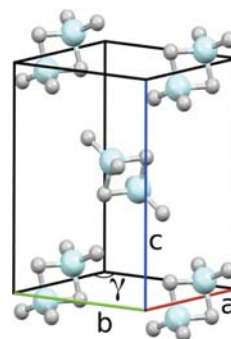


Figure 4. Structure of $P2_1/c$ (A) diborane at ambient pressure ($a = 4.519$ Å, $b = 4.725$ Å, $c = 8.874$ Å, $\gamma = 120.0^\circ$). The lattice parameters were optimized using the PBEsol functional.

Figure 5 shows the calculated Raman spectrum of $P2_1/c$ (A) diborane at 6.4 GPa along with the experimental spectrum of

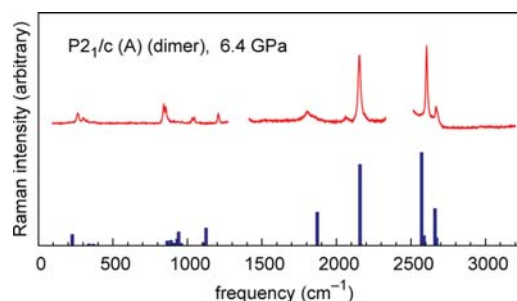


Figure 5. Experimental (red) and simulated (blue) Raman spectra of $P2_1/c$ (A) diborane at 6.4 GPa.

the sample taken at the same pressure.⁸ The experimental spectrum has two low-intensity lattice modes at 326 and 367 cm^{-1} which were not present at 4.2 GPa. These modes are found in the simulated spectrum of $P2_1/c$ (A) diborane at 340 and 370 cm^{-1} . The lattice mode observed at 265 cm^{-1} is no longer found in the simulated spectrum of β -diborane at 6.4 GPa but corresponds nicely to the peak at 227 cm^{-1} in the calculated spectrum of $P2_1/c$ (A) diborane. The calculated spectrum also contains a BH_2 twisting mode at 864 cm^{-1} , a BH_2 wagging mode at 931 cm^{-1} , and two low-intensity modes at 886 and 912 cm^{-1} . These correspond to the experimentally observed modes at 855, 907, 936, and 962 cm^{-1} .⁸ No other candidate structure has a Raman spectrum that matches experiment better than this (see Figure F2 and Table S2 in the Supporting Information).

The above evidence strongly suggests that phase II is $P2_1/c$ (A) diborane. The transition from β -diborane to this phase occurs around 6 GPa. Note that Yao and Hoffmann¹⁰ have previously identified $P2_1/c$ (A) diborane with the phase observed in 1925 by Mark and Pohland.⁵ We therefore propose that phase II observed by Muri and Song⁸ is the phase of Mark and Pohland. This is despite the fact that, according to the PBE calculations of Yao and Hoffmann¹⁰ and to our PBEsol calculations (Figure 2), $P2_1/c$ (A) diborane is slightly less stable than β -diborane, $P2_1/c$ (B) diborane, and the trimer structures at pressures between 1 and 80 GPa.

At pressures above 14 GPa, another phase transition was proposed in ref 8 to account for several subtle changes in the Raman spectrum. However, the experimental spectrum of diborane recorded at 14.1 GPa (after the proposed phase transition has occurred) is still well matched by the simulated spectrum of $P2_1/c$ (A) diborane (see Figure 6). Note that all three dimer structures considered in this work (β -diborane and the two $P2_1/c$ diboranes) have very similar internal vibration modes (see the Supporting Information), so their spectra differ mainly by the positions of lattice modes. The greatest discrepancy between the calculated and observed spectra of

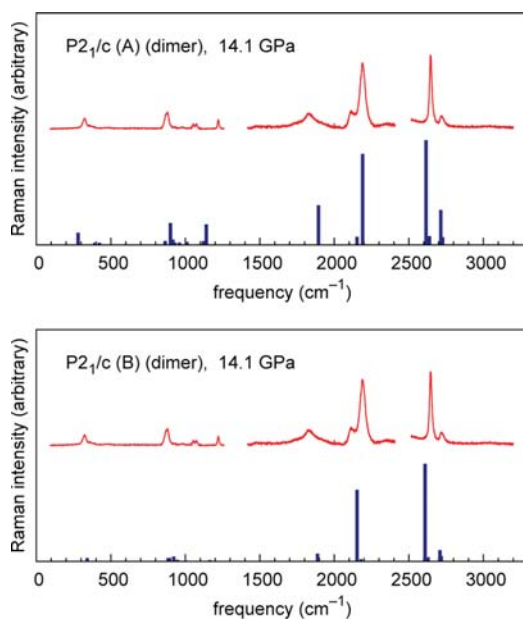


Figure 6. Experimental (red) and simulated (blue) Raman spectra of $P2_1/c$ (A) and $P2_1/c$ (B) diboranes at 14.1 GPa.

$P2_1/c$ (A) diborane at 14.1 GPa is in the position of the first lattice mode, which in our calculation occurs at 281 cm^{-1} , while the experimental one is at 323 cm^{-1} . This lattice mode is more closely matched in the simulated spectrum of $P2_1/c$ (B) diborane, where it occurs at 341 cm^{-1} . At 20.0 GPa, the first observed lattice mode shifts to 361 cm^{-1} , whereas the first lattice modes in the simulated Raman spectra of structures A and B are found at 298 and 359 (or possibly 337) cm^{-1} , respectively. Thus, if a phase transition above 14 GPa does take place, it is from $P2_1/c$ (A) diborane (phase II) to $P2_1/c$ (B) diborane (phase III). The structure of the latter is shown in Figure 7.

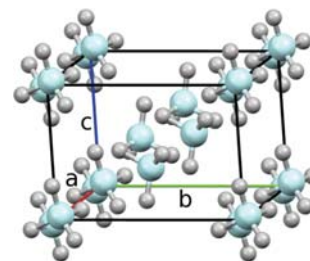


Figure 7. Structure of $P2_1/c$ (B) diborane at ambient pressure ($a = 4.577$ Å, $b = 6.954$ Å, $c = 4.998$ Å, $\gamma = 95.8^\circ$). The lattice parameters were optimized using the PBEsol functional.

To investigate the remaining possibility that the phase existing above 14 GPa consists of $(\text{BH}_3)_n$ units with $n > 2$, we calculated the Raman spectra of all candidate structures at 20.0 GPa and compared them to the experimental spectrum of the sample recorded at the same pressure (see Figure F4 in the Supporting Information). At 20.0 GPa, the simulated Raman spectrum of $P2_1/c$ (A) diborane remains the best match with experiment, although the $P2_1/c$ (B) structure cannot be ruled out. At the same time, the spectra of the trimer and linear chain structures are not even close to experiment. We conclude that the subtle changes in the observed Raman spectra of diborane above 14 GPa are most likely consequences of the compression of $P2_1/c$ (A), but allow for the possibility that $P2_1/c$ (A) diborane transforms near 14 GPa into $P2_1/c$ (B) diborane.

IR Spectra. To provide additional evidence supporting our structural assignments, we also simulated IR absorption spectra of compressed diborane and compared them to the published IR spectra from the Song group.⁹ Note that ref 9 did not report IR absorption data for frequencies below 800 cm^{-1} . Also, the broad band appearing above 3700 cm^{-1} in all experimental IR spectra of ref 9 is associated with overtones or combination modes,⁹ so it is absent from the simulated spectra which show only fundamental transitions.

The experimental IR spectrum recorded at 5.4 GPa is well matched by the simulated spectrum of β -diborane, as shown in Figure 8. The most intense peak in the simulated spectrum occurs at 1637 cm^{-1} , accompanied by a low-intensity mode at 1650 cm^{-1} . This pair matches the split band observed near 1600 cm^{-1} in the experimental spectrum. The internal ν_{14} and ν_{18} modes occur in the simulated spectrum at 930 and 1092 cm^{-1} , respectively, compared to 980 and 1176 cm^{-1} in the experimental spectrum. The simulated terminal BH symmetric stretching (ν_{16}) and antisymmetric BH stretching (ν_{18}) modes at 2565 and 2655 cm^{-1} likely correspond to the experimental peaks at 2598 and 2630 cm^{-1} , respectively. The high-intensity band at 2379 cm^{-1} is due to overtones/combination modes,⁹

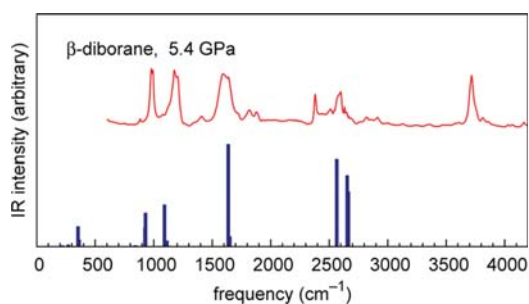


Figure 8. Experimental (red) and simulated (blue) IR spectra of β -diborane at 5.4 GPa.

so it is not present in the simulated spectrum. The simulated IR spectra of trimer and chain structures agree poorly with the experimental spectrum at 5.4 GPa (see Figure S5 in the Supporting Information). Thus, our simulated IR data are consistent with the conclusion that at 5.4 GPa diborane exists in the form of the β -phase (phase I).

Upon compression above 6 GPa, the best match between the calculated and experimental IR spectra is found for $P2_1/c$ (A) diborane (phase II), as was the case with the Raman spectra. The experimental and simulated spectra of $P2_1/c$ (A) diborane at 6.9 GPa are compared in Figure 9. The simulated spectrum

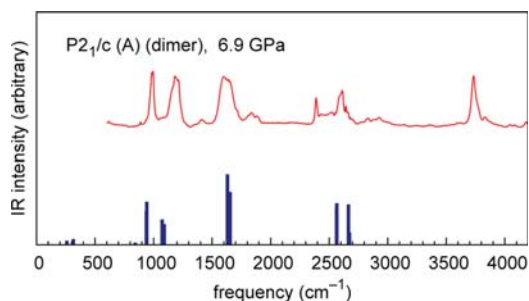


Figure 9. Experimental (red) and simulated (blue) IR spectra of $P2_1/c$ (A) diborane at 6.9 GPa.

reproduces most of the features noted in ref 9 including the evolution of a shoulder band of the ν_{18} mode near 1100 cm^{-1} and a more pronounced separation of the two peaks near 1630 cm^{-1} .

As in the Raman spectroscopic studies, the subtle differences between the experimental spectra taken at 6.9 GPa and above 14 GPa were interpreted by Song et al.⁹ as evidence of a polymorphic transition from phase II to phase III. These differences include⁹ the emergence of a new mode near 2760 cm^{-1} , development of an asymmetric profile of the ν_{14} mode near 1000 cm^{-1} , and an enhanced splitting of the ν_{18} mode near 1200 cm^{-1} . These changes are consistent with the simulated IR spectrum of $P2_1/c$ (A) diborane at 16.7 GPa and, to a lesser degree, with the spectrum of $P2_1/c$ (B) diborane (see Figure 10). The latter possibility cannot be ruled out because of the similarity between the IR spectra of these two structures.

IR spectra of crystalline triboranes and chain structures differ starkly from the experimental spectra recorded above 14 GPa (see Figures F7 and F8 in the Supporting Information). This again means that the high-pressure phases observed by the Song group are not oligomer or polymer structures. Thus, the spectral changes observed above 14 GPa are most likely consequences of compression of $P2_1/c$ (A) diborane. No other

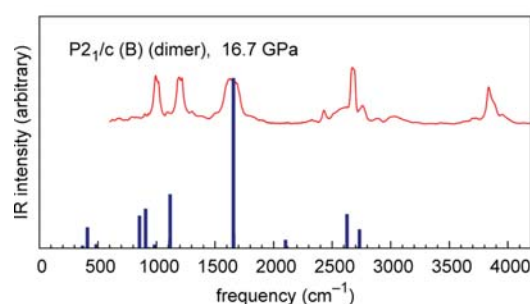
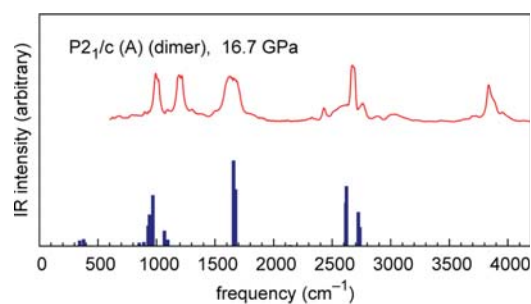


Figure 10. Experimental (red) and simulated (blue) IR spectra of $P2_1/c$ (A) and $P2_1/c$ (B) diboranes at 16.7 GPa.

polymorphic transitions between 14 and 24 GPa were observed or proposed in ref 9.

CONCLUSION

We have simulated the pressure dependence of Raman and IR spectra of 10 plausible crystalline structures of boron hydride for which experimental data^{8,9} are available. Comparison of the simulated spectra to the experiment shows that boron hydride exists as β -diborane (phase I) until about 6 GPa when it transforms into $P2_1/c$ (A) diborane (phase II). The subtle spectral changes above 14 GPa, which were previously interpreted by one of the authors^{8,9} as an indication of another phase transition, are attributed here to the compression of $P2_1/c$ (A) diborane. However, we do not rule out the possibility that near 14 GPa $P2_1/c$ (A) diborane is converted into $P2_1/c$ (B) diborane (phase III). This ambiguity is due to the fact that the simulated spectra of $P2_1/c$ (A) and $P2_1/c$ (B) diboranes are similar. What is certain is that none of the structures built up of $(\text{BH}_3)_n$ units with $n > 2$ has a vibrational spectrum that is consistent with the experimental observations reported in refs 8 and 9. Although the formation of cyclic oligomers and polymer chains is favored thermodynamically, it appears to be hindered kinetically. Our findings strongly agree with the conclusion of refs 8 and 9 that the geometry of the BHBH diborane ring is not altered significantly by compression and that B_2H_6 molecules remain chemically stable up to at least 24 GPa.

ASSOCIATED CONTENT

Supporting Information

(a) PBEsol lattice parameters of the 10 candidate structures optimized at ambient pressure; (b) observed and simulated LDA Raman spectra of the candidate structures at 4.2, 6.4, 14.1, and 20.0 GPa; (c) observed and simulated PBEsol IR spectra of the candidate structures at 5.4, 6.9, 16.7, and 20.6 GPa; (d) tables of observed and calculated LDA Raman shifts and intensities for selected candidate structures at 4.2, 6.4, 14.1, and 20.0 GPa; (e) tables of observed and calculated PBEsol IR

frequencies and intensities for selected candidate structures at 5.4, 6.9, 16.7, and 20.6 GPa. This material is available free of charge via the Internet at <http://pubs.acs.org>.

AUTHOR INFORMATION

Corresponding Author

*E-mail: vstarove@uwo.ca.

Notes

The authors declare no competing financial interest.

ACKNOWLEDGMENTS

A.T. thanks John Tse for helpful discussions. The calculations were performed using the facilities of the Shared Hierarchical Research Computing Network (SHARCNET) and Compute/Calcul Canada. The research was funded by the Ontario Ministry of Economic Development and Innovation through the Early Researcher Awards (ERA) Program.

REFERENCES

- (1) Lipscomb, W. N. *Boron Hydrides*; W. A. Benjamin: New York, 1963.
- (2) Laszlo, P. *Angew. Chem., Int. Ed.* **2000**, *39*, 2071.
- (3) Abe, K.; Ashcroft, N. W. *Phys. Rev. B* **2011**, *84*, 104118.
- (4) Barbee, T. W., III; McMahan, A. K.; Klepeis, J. E.; van Salfgaarde, M. *Phys. Rev. B* **1997**, *56*, 5148.
- (5) Mark, H.; Pohland, E. Z. *Kristallogr.* **1925**, *62*, 103.
- (6) Bolz, L. H.; Mauer, F. A.; Peiser, H. S. *J. Chem. Phys.* **1959**, *31*, 1005.
- (7) Smith, H. W.; Lipscomb, W. N. *J. Chem. Phys.* **1965**, *43*, 1060.
- (8) Murli, C.; Song, Y. *J. Phys. Chem. B* **2009**, *113*, 13509.
- (9) Song, Y.; Murli, C.; Liu, Z. *J. Chem. Phys.* **2009**, *131*, 174506.
- (10) Yao, Y.; Hoffmann, R. *J. Am. Chem. Soc.* **2011**, *133*, 21002.
- (11) Perdew, J. P.; Burke, K.; Ernzerhof, M. *Phys. Rev. Lett.* **1996**, *77*, 3865. Perdew, J. P.; Burke, K.; Ernzerhof, M. *Phys. Rev. Lett.* **1997**, *78*, 1396 (E).
- (12) Perdew, J. P.; Ruzsinszky, A.; Csonka, G. I.; Vydrov, O. A.; Scuseria, G. E.; Constantin, L. A.; Zhou, X.; Burke, K. *Phys. Rev. Lett.* **2008**, *100*, 136406.
- (13) Giannozzi, P.; Baroni, S.; Bonini, N.; Calandra, M.; Car, R.; Cavazzoni, C.; Ceresoli, D.; Chiarotti, G. L.; Cococcioni, M.; Dabo, I.; Dal Corso, A.; de Gironcoli, S.; Fabris, S.; Fratesi, G.; Gebauer, R.; Gerstmann, U.; Gougoussis, C.; Kokalj, A.; Lazzeri, M.; Martin-Samos, L.; Marzari, N.; Mauri, F.; Mazzarello, R.; Paolini, S.; Pasquarello, A.; Paulatto, L.; Sbraccia, C.; Scandolo, S.; Sclauzero, G.; Seitsonen, A. P.; Smogunov, A.; Umari, P.; Wentzcovitch, R. M. *J. Phys.: Condens. Matter* **2009**, *21*, 395502 <http://www.quantum-espresso.org>.
- (14) Vanderbilt, D. *Phys. Rev. B* **1990**, *41*, 7892.
- (15) Monkhorst, H. J.; Pack, J. D. *Phys. Rev. B* **1976**, *13*, 5188.
- (16) Lazzeri, M.; Mauri, F. *Phys. Rev. Lett.* **2003**, *90*, 036401.
- (17) Baroni, S.; de Gironcoli, S.; Dal Corso, A.; Giannozzi, P. *Rev. Mod. Phys.* **2001**, *73*, 515.
- (18) Kokalj, A. *Comput. Mater. Sci.* **2003**, *28*, 155 <http://www.xcrysden.org>.